PROPAGATION OF CRAZING IN VISCOELASTIC MEDIA*

Z. D. Zhang, S. S. Chern and C. C. Hsiao
Department of Aerospace Engineering and Mechanics
University of Minnesota, Minneapolis, MN 55455

Up to now, the growth rate of a craze has been considered either constant or inversely proportional to time. By taking into consideration the effect of the surrounding population of crazes, it is found that the craze growth rate is affected by the local effective stress acting in the vicinity of the craze. Measured data of craze length as a function of time are found to be greatly affected by local interactions.

(NASA-CR-173244) PROPAGATION OF CRAZING IN VISCOELASTIC MEDIA (Minnesota Univ.) 40 p
HC A03/MF A01 CSCL 20K

N84-16583

Unclas
G3/39 10143

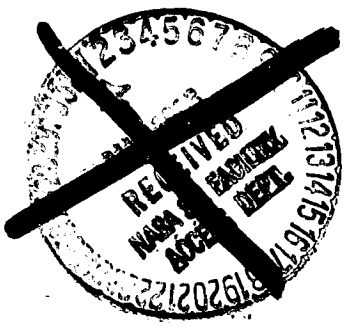

*Supported in part by NASA NAG 1-278

I. INTRODUCTION

In response to a tensile stress glassy polymers can exhibit crazing which is a phenomenon of considerable practical and theoretical importance in the use of many plastics. Since the first important paper [1] dealing with the craze was published, a great deal of knowledge has been accumulated on the development of crazing in glassy polymers in a tensile stress field [2-9]. For predicting craze growth in polycarbonate, Verheulpen-Heymans and Bauwens [7] have presented a two-dimensional model for craze growth. They obtained that the craze length varies linearly with respect to the log of time and hence craze growth velocity decreases as time increases, in good agreement with their experimental result under constant uniaxial tensile load. Argon et al [8] have proposed new mechanisms for craze initiation and growth. In their model, the craze growth velocity is assumed to be proportional to the constant craze tip opening velocity. Then they conclude that the craze length increases linearly with time. They also get good agreement between theoretical and experimental results on PMMA and PS.

It has been pointed out that both of the above models were somewhat similar in many ways and contained similar limitations. While they satisfy specific data but are incompatible and neither are capable of predicting the effect of craze interactions [10].

Recently, a time dependent theory of crazing behavior on polymers [11] based upon linear viscoelasticity theory and first law of thermodynamics for predicting the craze length as a function

of time, has found that a craze may propagate with increasing velocity for a thin sheet of viscoelastic medium which contains a single craze under uniaxial creep conditions.

It is difficult to draw conclusions for one against the others, because there are several potential sources of discrepancy among the results of [7], [8] and [11] such as tensile stress applied, material used and environment exposed. However, an important factor which may dominate craze growth behavior is the interaction of the neighboring crazes.

In this paper, an attempt is made to demonstrate how craze growth behavior is affected by the craze density (which is defined as the total number of crazes per unit surface area) surrounding that craze. The measured craze length as a function of time will be compared with some calculated results of PS at room temperature.

II. EXPERIMENTAL

As shown in Figure 1, the development of multi-crazes in a simple tension specimen is usually on the surfaces of the specimen. In order to measure the changing length of the crazes, an experimental set up for determining the craze tip position and thus the craze length as a function of time is constructed. Sheet specimens of polystyrene with a neck region have been cut and secured onto the clamps of a creep testing machine for loading. As shown in Figure 2 while the specimen was being stressed, a microscope was used for viewing the surface conditions of the stressed specimen. Using a He-Ne laser the surface crazing was projected onto an image screen for observation and measurement. All the creep tests were conducted at a constant room temperature of 21°C under a constant applied load. Usually a short period of time elapsed before crazes occurred. Starting at this craze initiation time the craze lengths were monitored. The craze lengths were enlarged 400 times and measured to 0.1 mm at regular intervals with the aid of a travelling microscope.

The eight inch-long specimens were cut from a 10-mil thick biaxially oriented polystyree sheet. The gage section was half inches wide and two inches long. Under load after inception of crazing, the number of crazes (per unit area) as well as the lengths of individual crazes were observed to increase. Figure 3 shows the total number of craze per unit area as a function of time for a typical specimen under the load corresponding to a creep stress of 34.4 N/mm^2 at the gage section. Figure 4 shows the increase in the individual craze lengths as time increases.

Biaxially oriented polystrene specimens were used because of the ease of developing the crazes. The density of the craze was found to be adequate for quantitative considerations. During the course of this investigation sufficiently large areas have been taken to insure the statistical representation of the crazing behavior. It was recognized that both the lengths and the number of crazes increase as a function of time. As shown in Figure 5, in a local region, out of many crazes, four were selected for identifying a common behavior. The craze lengths were plotted as a function of time. The similarity of their behavior is quite clear. More interesting is that by normalizing the craze length (current craze length divided by its initial length) all the individual curves reduce to a single one. This is shown in Figure 6, a single master curve characterizes the time dependent behavior of all the crazes developed in that region. In other words this single master curve represents the typical behavior of a family of crazes in a local neighborhood under a specific loading situation as stated earlier.

III. REDUCTION OF THE MULTI-CRAZE PROBLEM

Among all the parameters describing the crazing phenomenon, two important ones are the total number of crazes appearing on the surface of the stressed medium $N(t)$ at time t and the length of each (ith) individual craze $c_i(t)$. The former is associated with the craze initiation while the latter is related to craze growth. Both parameters are highly dependent on the viscoelastic behavior of the media.

In dealing with crazing, like any other physical or mechanics problems, continuum models are utilized. Aside from the regular field equations such as equations of motion and kinematic relations the system must obey at all times during the development of crazing the fundamental principle of the global conservation of energy. The rate of work done by external forces and all energies that enter or leave the material body containing crazes per unit time must equal the time rate of change of the internal and kinetic energies plus the energies associated with the formation of crazes, excluding chemical, electrical, etc. energies except heat. On this basis the global conservation of energy per unit time for a crazed viscoelastic medium containing $N(t)$ number of crazes at any time t becomes

$$\dot{W}(t) = \dot{E}(t) + \dot{D}(t) + \dot{K}(t) + \overline{\sum_{i=1}^{N(t)} \xi_i(t)}^{\cdot}, \tag{1}$$

where $W(t)$ is the mechanical work done by external load,

$E(t)$ is the stored elastic strain energy of the uncrazed portion of the medium,

$D(t)$ is the dissipated energy by the uncrazed portion of the medium,

$K(t)$ is the kinetic energy of the uncrazed medium.

and

$\xi_i(t)$ is the total energy absorbed by the ith craze developed in the medium from the beginning of craze initiation to current time t.

In the case of relaxation it is expected that the external work done $W(t)$ approaches a constant value initially. The energy required for the inception and propagation of the crazes comes from the release of the stored elastic strain energy $E(t)$. In the case of creep both the stress and strain increase and the external work increases continuously which provides energy for the initiation and propagation of crazing. Each craze is an energy sink which absorbs and dissipates energy from its own neighborhood. The energy absorbed $\xi_i(t)$ by the ith craze is characterized by the development of the craze through the release of the elastic energy in the surrounding medium.

In what follows is an attempt to reduce the problem containing multi-crazes to one dealing with only one representative craze.

Originally the whole specimen is a region subjected to an external stress σ_o, the medium is homogeneous, there is no new phase created until crazes are developed. After the development of the new phases, subregions may be considered according to the number of crazes developed in that region.

At any subregion it appears reasonable to consider that the number of crazes developed will be proportional to the energy

available in that subregion. If $\sigma_e(x,z,t)$ and $\dot{\varepsilon}_e(x,z,t)$ are respectively the effective stress and the strain rate for the subregion, the energy available per unit volume at time t will be:

$$\int_o^t \sigma_e(x,z,\tau)\dot{\varepsilon}_e(x,z,\tau)d\tau . \tag{2}$$

Since crazes are sources of energy sinks, several hundred times the amount of energy will be needed for the initiation of a single craze [information will be published elsewhere] as compared with that for the elastic deformation of the medium of the craze size, essentially the craze density $n(x,z,t)$ in this subregion will be proportional to the energy given in (2), that is

$$\int_o^t \sigma_e(x,z,\tau)\dot{\varepsilon}_e(x,z,\tau)d\tau \sim n(x,z,t) . \tag{3}$$

In the case of creep, $\dot{\varepsilon}_e(x,z,t)$ is a constant after a transient period, then differentiation of (3) with respect to time yields:

$$\dot{\varepsilon}_e\sigma_e(x,z,t) \sim \dot{n}(x,z,t), \tag{4}$$

or

$$\sigma_e(x,z,t) \sim \dot{n}(x,z,t) . \tag{5}$$

With this important relation established, the computation of the time dependent craze length will be greatly simplified provided that $n(x,z,t)$ is predetermined.

IV. CONSIDERATIONS OF CRAZE PROPAGATION

Assuming that each craze has basically the same configuration as any other craze then by referring to a central fixed (x,z) coordinate system, an idealized symmetrical craze in a tensile local effective stress field $\sigma_e(t)$ is shown in Figure 7. By taking into consideration the time dependent nature of both the polymer medium and the craze, a craze length is designated by 2c(t) at time t and the time dependent stresses and displacements are shown in Figure 8. The half vertical distance between the two craze surfaces will be called the craze opening displacement and denoted by w(x,t). The craze fibril domains are formed by continuous drawing from the unoriented bulk polymer. This drawing process cuases the material mass to flow from the original polymer into a highly oriented new phase. The stress acting on the interface may be called the craze envelope stress with notation $\sigma_c(x,t)$ which is time dependent. The general state of stress in the bulk polymer is designated by $\sigma(x,z,t)$.

The idealized craze structure has been considered as cylindrical domains of fibrils of diameter $\delta_f(x,t)$, which ma be different from position to position. During the crazing process the diameter of each fibril domain may also change with time as its length changes. Each fiber sustains a stress $\sigma_f(x,t)$ which may be different from the craze envelope stress $\sigma_c(x,t)$. The former represents the true fibril domain stress while the latter is an average stress usually referred to as an engineering stress by taking the fiber domains and the voids altogether into consideration. Thus the ratio $\sigma_f(x,t)/\sigma_c(x,t) = \lambda(x,t)$ equals the draw ratio of the fibril domains within any craze. Its inverse is the

volume fraction V_f. The actual fibril distribution density function $n_f(x,t)$ is defined as the number of load bearing fibrils passing through a normal unit area in the craze plane at time t. The volume fraction of fibrils $V_f(x,t)$ inside an individual craze is equal to $\frac{\pi}{4}\,\delta_f^2(x,t)\,n_f(x,t)$.

The absorbed energy $\xi(t)$ nucleates and creates fibril domains near the craze tip and transforms more material mass from the original phase into the new phase of oriented fibril domains, void formations and further deformations as well as possible microfractures of the highly oriented fibrils. The local energy balance equation per unit time for a craze at time t may be expressed as an energy rate balance equation with dot representing the time derivative:

$$\dot{\xi}(t) = \dot{\Gamma}_c(t) + \dot{\Gamma}_f(t) + \dot{D}_f(t) + \dot{E}_f(t) + \dot{K}_f(t), \qquad (6)$$

where Γ_c is the energy required to nucleate the fibril domains near the craze tips,

Γ_f is the total surface free energy of domain fibrils contained in the craze,

$D_f(t)$ is the total dissipated energy contained in the domain of fibrils of the craze,

$E_f(t)$ is the stored strain energy contained in the domain of fibrils inside the craze,

and

$K_f(t)$ is the kinetic energy of the domain of fibrils contained in the craze.

Associated with any craze, Γ_f, D_f, E_f and K_f can be expressed in terms of more elementary parameters as follows:

$$\Gamma_f(t) = 4 \int_o^{c(t)} \pi \delta_f(x,t) \gamma_f n_f(x,t) w(x,t) dx.$$

$$E_f(t) = 4 \int_o^{c(t)} \frac{\pi}{4} \delta_f^2(x,t) e_f(x,t) n_f(x,t) w(x,t) dx.$$

$$D_f(t) = 4 \int_o^{c(t)} \frac{\pi}{4} \delta_f^2(x,t) d_f(x,t) n_f(x,t) w(x,t) dx.$$

$$K_f(t) = 4 \int_o^{c(t)} \frac{\pi}{4} \delta_f^2(x,t) k_f(x,t) n_f(x,t) w(x,t) dx.$$

where γ_f is the surface free energy per unit surface area of the fibril domain, this energy density is assumed to be a material constant.

e_f, d_f, and k_f are respectively the elastic strain energy, the dissipative energy and the kinetic energy per unit volume of the fibril domain.

Since the fibril domain nucleation rate at the craze tip must be proportional to the craze growth velocity $\dot{c}(t)$, hence the energy required to nucleate the fibril domains near the craze tip per unit time becomes:

$$\dot{\Gamma}_c = 4\beta_c \dot{c}(t). \tag{7}$$

where β_c is assumed to be a constant.

The energy absorption rate of a craze $\dot{\xi}(t)$ can be obtained by performing integration of the product of the craze envelope stress $\sigma_c(x,t)$ and the craze opening velocity

$\dot{w}(x,t)$ along the craze length, i.e.

$$\dot{\xi}(t) = 4 \int_0^{c(t)} \sigma_c(x,t) \frac{\partial w(x,t)}{\partial t} dx \tag{8}$$

Taking the derivatives of $\Gamma_f(t)$, $E_f(t)$, $D_f(t)$ and $K_f(t)$ and combining with (6), (7) and (8), one obtains the following equation which governs the individual craze length $c(t)$ as a function of time t:

$$\int_0^{c(t)} \{\sigma_c(x,t) \frac{\partial w(x,t)}{\partial t} - \frac{\partial}{\partial t} [\beta_f(x,t) V_f(x,t) w(x,t)]\} dx$$

$$= \beta_c \dot{c}(t). \tag{9}$$

where

$$V_f \equiv \frac{\pi}{4} \delta_f^2(x,t) n(x,t). \tag{10}$$

and

$$\beta_f(x,t) = \frac{4\gamma_f}{\delta_f(x,t)} + [e_f(x,t) + d_f(x,t) + k_f(x,t)]. \tag{11}$$

Equation (9) is a nonlinear differential-integral equation of $c(t)$ involving five parameters σ_c, w, V_f, β_f and β_c which form the basis to characterize each individual craze. This equation is not only describing the steady-state craze growth, but also governing the craze-crack transition. Once a crack is formed within the craze, (9) can be used to predict the crack propagation as a special case.

Among all the parameters involved in equation (9), most of them are associated with intrinsic material properties which are insensitive to the geometry of the craze and to the interaction of neighboring crazes. For example, at the time well before craze-crack transition, to a first approximation, one may assume that the load-bearing fiber volume fraction $V_f(x,t)$ and the fiber diameter $\delta_f(x,t)$ are constants both in position x and time t during crazing process. It may also be assumed that the kinetic energy K_f, dissipative energy D_f and the elastic strain energy E_f are negligible compared with the other energy term, namely the phase transformation energy $4\gamma_f/\delta_f$. Then (9) reduces to the following form:

$$\beta_c \dot{c}(x,t) = \int_0^{c(t)} h(x,t) \frac{\partial w(x,t)}{\partial t} dx, \tag{12}$$

where

$$h(x,t) \equiv \sigma_c(x,t) - \beta_f V_f, \tag{13}$$

and

$$\beta_f \equiv 4 \frac{\gamma_f}{\delta_f}$$

which may be regarded as the energy required to rearrange a unit volume of the original medium into the new phase composed of oriented fibril domains. Equation (12) has the meaning that the craze growth rate $\dot{c}(t)$ is proportional to the weighted average of the craze opening velocity $\dot{w}(x,t)$ with weighting function $h(x,t)$ as defined in (13). Physically (12) may be visualized as the craze growth criterion derived from the first law of thermodynamics. Therefore, it is not surprising that (12) should be more general than the craze growth criteria used in [7] and [8]. As we have mentioned

earlier in the introduction of this paper, Verheulpen-Heymans and Bauwens [7] obtained their craze growth criterion by assuming that the ratio of the craze opening at center ($x = o$) to the craze length $c(t)$ be kept constant during the crazing process. This can be expressed in the following mathematical form in terms of our terminologies:

$$\frac{w(o,t)}{c(t)} = \gamma_1 = \text{constant}. \tag{14}$$

By taking the derivative with respect to time t, one can rearrange (14) in the form:

$$\gamma_1 \dot{c}(t) = \dot{w}(c,t). \tag{15}$$

Comparing (15) with (12), one can easily see that (15) is a special case of (12) when the weighting function $h(x,t)$ in (12) is reduced to:

$$h(x,t) = \delta(x), \tag{16}$$

where $\delta(x)$ is the Dirac-delta function.

On the other hand, in order to take the strain rate behavior into consideration for the craze growth criterion, Argon and Salama [8] assumed that the craze growth rate is linearly proportional to the strain rate of the craze at the position $a(t)$ which is at some point between the center $x = o$ and the craze tip $x = c(t)$. This can also be expressed as follows:

$$\gamma_2 \dot{c}(t) = \dot{w}(a(t),t), \qquad o \leq a(t) < c(t), \tag{17}$$

where γ_2 is a constant.

Once again (17) is seen to be a special case of (12) simply by taking the weighting function $h(x,t)$ as a delta function that

$$h(x,t) = \delta(a(t)). \tag{18}$$

Now equation (12) is a nonlinear differential-integral functional equation of the form [see Appendix A]:

$$f(\dot{c}(t),\ c(t),\ \sigma_o,\ \beta_c,\ \beta_f,\ V_f,\ J(t),\ t) = 0 \tag{19}$$

which is applicable for any specific applied stress σ_o. Among all the arguments, $c(t)$ and $\dot{c}(t)$ are being sought, σ_o can be selected, β_c, β_f, and V_f must be experimentally determined, $J(t)$ can be measured and t is an independent variable. Other qualtities such as $w(x,t)$ must be obtained first before $c(t)$ is evaluated. Some further considerations are also given below in connection with the analysis of this craze propagation.

V. FURTHER CONSIDERATIONS OF CRAZE PROPAGATION

In order to obtain c(x,t), w(x,t) in (12) must be obtained first. To determine w(x,t) the field equations governing the quasi-equilibrium and compatibility conditions must be solved together with the constitutive behavior of the viscoelastic media subject to proper initial and boundary restrictions.

Using the classical correspondence principle developed in linear viscoelasticity and molecular orientation theory [12] the craze opening displacement for a single craze in viscoelastic medium has been presented previously [11] and the results will be recalled briefly here:

$$w(x,t) = \frac{\lambda}{\lambda-1}\left[C_b(0)\phi(x,t) + \int_0^t \dot{C}_b(t-\tau)\phi(x,\tau)d\tau\right], \tag{20}$$

where

$$\phi(x,t) = \frac{2}{\pi}\int_x^{c(t)} \frac{\eta g(\eta,t)}{\sqrt{(\eta^2-x^2)}}\,d\eta, \tag{21}$$

$$g(\eta,t) = \int_0^{\eta} \frac{\sigma_e(t) - \sigma_c(x,t)}{\sqrt{(\eta^2-x^2)}}\,dx\ , \tag{22}$$

and

$$C_b(t) \equiv \mathcal{L}^{-1}\,\frac{1-s^2\bar{\nu}^2}{s^2\bar{E}(s)} = \mathcal{L}^{-1}\,\frac{2(1-\nu^2)}{s^2\bar{E}(s)}\ , \tag{23}$$

in which the bar denotes the Laplace transform of a function of time, into a function in the LaPlace domain in s, i.e.

$$\bar{F}(s) = \int_0^{\infty} e^{-st}F(t)\,dt, \tag{24}$$

where $\mathcal{L}^{-1}$ denotes the inversion of the Laplace transform and ν,E are respectively the Poisson's ratio, and the elastic modulus of the original unoriented bulk polymer. λ is the natural draw ratio of the craze fibril domain.

The craze envelope stress $\sigma_c(x,t)$ in (22) usually depends upon both position and time. Based upon a number of previous results [9, 11, 13], the stress $\sigma_c(x,t)$ to a first approximation can be taken as follows:

$$\sigma_c(x,t) = \sigma_1(t) \quad \text{for} \quad o \leq |x| < a(t)$$

$$\sigma_c(x,t) = \sigma_2(t) \quad \text{for} \quad a(t) \leq |x| \leq c(t). \tag{25}$$

where a(t) separates the stresses $\sigma_1(t)$ and $\sigma_2(t)$ which are both functions of time. It has been shown that the use of the two-step stress distribution [9, 11, 13] results in excellent approximation as compared with actual findings.

In addition, the introduction of step functions in the stresses should reduce tremendously the mathematical complicities and computations. This has been evidenced by the recent report on a time dependent theory of crazing behavior in polymers [11].

Because the craze envelope stress $\sigma_c(x,t)$ must balance the effective stress $\sigma_e(t)$ at all times in such a way that the stress field within the uncrazed medium is finite everywhere (i.e. there are no stress singularities), then a(t) can be determined by the following condition[11]:

$$\int_o^{c(t)} \frac{\sigma_c(x,t)}{(c^2(t)-x^2)^{1/2}}\, dx = \frac{\pi}{2}\sigma_e(t). \tag{26}$$

By considering $\sigma_1(t)$ and $\sigma_2(t)$ as follows:

$$\sigma_1(t) = \alpha_1 \sigma_e(t),$$

$$\sigma_2(t) = \alpha_2 \sigma_e(t), \tag{27}$$

where α_1, α_2 are constants, indeed the solution of (12) is greatly simplified. According to the experimental results in PS the stress $\sigma_1(t)$ is about 10% below the applied stress along the majority of its length and 15% above the applied stress for $\sigma_2(t)$ around the craze tip [14].

Substituting (27) into (26) and solving:

$$a(t) = c(t)\cos\theta, \tag{28}$$

where

$$\theta = \frac{\pi}{2} \frac{\sigma_e(t)-\sigma_1(t)}{\sigma_2(t)-\sigma_1(t)} = \frac{\pi}{2} \frac{1-\alpha_1}{\alpha_2-\alpha_1} \quad . \tag{29}$$

With respect to the time dependent craze density $n(t)$ based upon experimental measurements at the location where craze lengths were monitored, the following equation was found to be quite adequate for representing the craze population as a function of time:

$$n(t) = A(1-e^{-Bt}). \tag{30}$$

where A and B are constants. For polystyrene, referring to Figure 3, A was found to be 78 and B = 0.4.

According to the linear relationship between the effective stress $\sigma_e(t)$ and $\dot{n}(t)$, [see Equation (5)], the following equation can be established for creep:

$$\sigma_e(t) = Ce^{-Bt} + D \tag{31}$$

where C and D are again constants determinable by the initial condition that $\sigma_e(0) = \sigma_o$, and that the weighting function in (13) must be positive definite. On this basis, C has been found to be 4.7 N/mm^2 and D = 29.7 N/mm^2, for polystyrene under the tensile stress σ_o = 34.4 N/mm^2. This reflects the correct physical picture that initially no craze exists and the medium is homogeneous. After crazes develop the craze envelope stress $\sigma_c(x,t)$ must always be greater than the craze transformation energy $\beta_f V_f$ as shown in (13). Otherwise craze will not occur or propagate.

Apparently, information concerning the interactions among neighboring crazes can be effectively taken care of through the application of the effective stress $\sigma_e(t)$ as a function of the rate of change of the local craze number.

VI. RESULTS

Using computer aided numerical methods (A15) a reduced form of (A1) or (19) or (12) has been solved. For polystyrene, only three constants are now needed. They are

$$\beta_c = 0.7 \times 10^{-6} \text{ J/mm}^2$$

$$\beta_f = 0.112 \text{ J/mm}^3$$

and $$V_f = 1/4$$

These values are obtained on the basis that $\delta_f = 15$ nm, $\gamma_f = 0.42 \cdot 10^{-6}$ J/mm^2 and $\lambda = 4$ which have been experimentally found [15]. Note that $V_f \equiv 1/\lambda$. Using these together with the creep compliance $J(t)$ as determined in (B2) Appendix B, the following results have been obtained.

The craze envelope stress distribution $\sigma_c(x,t)$ for polystyrene is given in Figure 9 for a specific craze of length just below 150 μm. Based upon various considerations, as stated before, a fairly accurate craze propagation behavior should prevail if all the subregional crazes are consistently stressed. Indeed this is the case, the computed time dependent craze length is given in Figure 10 in which one normalized curve is shown to represent the typical craze length-time behavior. Compared with the experimental data as shown in Figure 6, a fairly good agreement with the calculated results is obtained.

It may be quite significant that the time dependent single craze length in a viscoelastic medium has been found to propagate to infinity in a finite time if only one craze is considered [11].

According to the current analysis, when craze interactions are taken into consideration, however, the craze length as a function of time propagate to a finite value as time goes to infinity.

VII. DISCUSSION

(1) Craze Propagation

The craze propagation computed analytically agrees fairly well with the experimental results (Figure 10). It was found that the craze growth is decelerated with time. This means that the craze length increases with time and its velocity decreases with time. From Equation (12), it is observed that craze arrest ($\dot{c} = 0$) occurs when either $\sigma_c = \beta_f V_f$ or $\partial w(x,t)/\partial t = 0$. The former occurs when the energy absorption rate by crazing is used up for drawing new fibrils out of the matrix, while the latter is possible only if molecular entanglements enhance the stiffness of the fibril domain such that further opening becomes difficult.

(2) Craze Number

As shown in Figure 11 it was found that the number and length of crazes developed in creep are strongly dependent on the magnitude of the external load. At high stresses a large number of small crazes become visible after a relatively short time, while under small stresses a small number of large crazes become visible after a long loading time.

(3) Local Effective Stress and Rate of Craze Number

It is interesting to note that the local effective stress is linearly associated with the rate of change of the local craze number. This relationship seems to be quite useful for analyzing craze interactions.

APPENDIX A

On Craze Length c(t)

By substituting (25) and (27) into (12) one obtains:

$$[\alpha_1\sigma_e(t) - \beta_f V_f] \int_o^{a(t)} \frac{\partial w(x,t)}{\partial t}\, dx$$

$$+ [\alpha_2\sigma_e(t) - \beta_f V_f] \int_{a(t)}^{c(t)} \frac{\partial w(x,t)}{\partial t}\, dx = \beta_c \dot{c}(t). \tag{A1}$$

Further, by substituting (25) and (27) into (21) and (22), $\phi(x,t)$ is found as follows:

$$\phi(x,t) = \frac{1}{\pi}(\alpha_2-\alpha_1)\sigma_e(t)\left[(x+\gamma c(t))\cosh^{-1}\frac{c(t)+\gamma x}{x+\dot{c}(t)}\right.$$

$$\left. - (x-\gamma c(t))\cosh^{-1}\frac{c(t)-\gamma x}{x-\gamma c(t)}\right], \tag{A2}$$

where

$$\gamma = \cos\theta,$$

$$\phi(x,t)\Big|_{x=a(t)} = (\alpha_2-\alpha_1)\sigma_e(t)c(t)I_2. \tag{A3}$$

with

$$I_2 = \frac{2}{\pi}\cos\theta \ln\sec\theta. \tag{A4}$$

$$\int_0^{a(t)} \phi(x,t)dx = (\alpha_2-\alpha_1)\sigma_e(t)c^2(t)I_1, \tag{A5}$$

where

$$I_1 = \cos^2\theta\left(\frac{1}{2}\tan\theta - \frac{\theta}{\pi}\tan\theta + \frac{2}{\pi}\ln\sec\theta\right). \tag{A6}$$

$$\int_{a(t)}^{c(t)} \phi(x,t)dx = (\alpha_2-\alpha_1)\sigma_e(t)C^2(t)I_3, \tag{A7}$$

where

$$I_3 = \frac{1}{\pi}\cos^2\theta(\theta\tan\theta - 2\ln\sec\theta). \tag{A8}$$

$$\frac{d}{dt}\int_0^{a(t)} \phi(x,t)dx = (\alpha_2-\alpha_1)\left[\dot{\sigma}_e(t)c^2(t) + 2\sigma_e(t)c(t)\dot{c}(t)\right]I_1, \tag{A9}$$

$$\frac{d}{dt}\int_{a(t)}^{c(t)} \phi(x,t)dx = (\alpha_2-\alpha_1)\left[\sigma_e(t)c^2(t) + 2\sigma_e(t)c(t)\dot{c}(t)\right]I_3 . \tag{A10}$$

Using the above results and (20), one gets the following:

$$\int_0^{a(t)} \frac{\partial w(x,t)}{\partial t}dx = \frac{\lambda}{\lambda-1}\{[C_b(0)I_1\dot{\sigma}_e(t)c^2(t)$$

$$+ C_b(0)(2I_1-I_2)\sigma_e(t)c(t)\dot{c}(t) + C_b(0)I_1\sigma_e(t)c^2(t)]\cdot$$

$$(\alpha_2-\alpha_1) + R_1(t)\}, \tag{A11}$$

$$\int_{a(t)}^{c(t)} \frac{\partial w(x,t)}{\partial t} dx = \frac{\lambda}{\lambda-1} \{ [C_b(0) I_3 \dot{\sigma}_e(t) c^2(t)$$

$$+ C_b(0)(2I_3+I_2)\sigma_e(t) c(t) \dot{c}(t) + \dot{C}_b(0) I_3 \sigma_e(t) c^2(t)] (\alpha_2-\alpha_1)$$

$$+ R_2(t) \}, \qquad \text{(A12)}$$

where

$$R_1(t) = \int_o^{a(t)} \int_o^t \ddot{C}_b(t-\tau)\phi(x,\tau) d\tau dx, \qquad \text{(A13)}$$

$$R_2(t) = \int_{a(t)}^{c(t)} \int_o^t \ddot{C}_b(t-\tau)\phi(x,\tau) d\tau dx, \qquad \text{(A14)}$$

and λ is the fibril draw ratio. Substituting (A11) and (A12) into (A1), finally one obtains:

$$\dot{c}(t) = \frac{K_1(t) c^2(t) + K_2(t)}{\beta_c - K_3(t) c(t)}, \qquad \text{(A15)}$$

where

$$K_1(t) = \frac{\lambda}{\lambda-1}(\alpha_2-\alpha_1)[C_b(0)\dot{\sigma}_e(t) + \dot{C}_b(0)\sigma_e(t)] \cdot$$

$$[I_1 L_1(t) + I_3 L_2(t)] \qquad \text{(A16)}$$

$$K_2(t) = \frac{\lambda}{\lambda-1}[L_1(t) R_1(t) + L_2(t) R_2(t)] \qquad \text{(A17)}$$

$$K_3(t) = \frac{\lambda}{\lambda-1}(\alpha_2-\alpha_1) C_b(0) [(2I_1-I_2) L_1(t) + (2I_3+I_2) L_2(t)] \sigma_e(t), \qquad \text{(A18)}$$

with

$$L_1(t) = \alpha_1 \sigma_e(t) - \beta_f V_f, \qquad \text{(A19)}$$

$$L_2(t) = \alpha_2 \sigma_e(t) - \beta_f V_f. \qquad \text{(A20)}$$

APPENDIX B

On Creep Compliance J(t)

Before any calculation can be accomplished, the constitutive behavior of the medium in creep must be obtained and properly represented for computation.

Taking the experimental polystyrene sheet as an example, Figure 12 shows the experimentally measured creep compliance J(t). The quantity $C_b(t)$ is closely related to this creep compliance. By assuming for polystyrene that the Poisson's ratio $\nu = 0.395$, a constant, then

$$C_b(t) = \mathcal{L}^{-1} \frac{2(1-\nu^2)}{s^2\bar{E}(s)} = 2(1-\nu^2)\mathcal{L}^{-1}\,\bar{J}(s) = 2(1-\nu^2)J(t). \tag{B1}$$

For any arbitrary times, a very good approximation may be obtained using a linear viscoelastic spectrum form[16]:

$$J(t) = J_0 + \sum_{i=1}^{m} J_i(1-e^{-t/\tau_i}) \tag{B2}$$

where J_i's and τ_i's are respectively constant material compliances and retardation times. With the measured creep compliance curve available, these quantities can be obtained using a curve fitting technique.

For polystyrene under the creep stress $\sigma_o = 34.4$ N/mm , the following data are found to represent a close fit:

$m = 4$

J_i's	τ_i's
$J_0 = 0.307 \times 10^{-3}\ mm^2/N$	$\tau_1 = 1.0/h,$
$J_1 = 0.071 \times 10^{-3}\ mm^2/N$	$\tau_2 = 10.0/h,$
$J_2 = 0.062 \times 10^{-3}\ mm^2/N$	$\tau_3 = 80.0/h,$
$J_3 = 0.045 \times 10^{-3}\ mm^2/N$	$\tau_4 = 110.0/h,$
$J_4 = 0.031 \times 10^{-3}\ mm^2/N$	

REFERENCES

1. C. C. Hsiao, J. A. Sauer, J. Appl. Phys. 21, 1071, (1950).
2. M. I. Bessenov and E. V. Kuvshinskii, Sov. Phys. Solid State, 3, 950 (1961).
3. J. A. Sauer and C. C. Hsiao, Trans. ASME, 75, 895, (1953).
4. I. Narisawa and T. Knodo, J. Polymer Sci. Phys. 11, 223, (1973).
5. N. V. Heymans and J. C. Bauwens, J. Mater. Sci. 11, 1, (1976).
6. J. G. WIlliams, "Advance in Polymer Science", 27, 69, Springer Verlag, Heidelberg, (1978).
7. N. Verheulpen-Heymans and J. C. Bauwens, J. Mater. Sci. 11, 7, (1976).
8. A. S. Argon and J. G. Hannoosh, Phil. Mag. 36, 1195, (1977); A. S. Argon and M. M. Salama, Phil. Mag. 36, 1217, (1977).
9. B. D. Lauternasser and E. J. Kramer, Phil. Mag. A 39, 469, (1979).
10. N. J. Mills, J. Mater. Sci., 16, 1317 and 1332 (1981).
11. S. S. Chern and C. C. Hsiao, J. Appl. Phys., 53, 6541, (1982).
12. C. C. Hsiao, J. Appl, Phys. 30, 1492, (1959).
13. L. Bevan, J. Appl. Polymer Science, 27, 4263, (1982).
14. A. M. Donald and E. J. Kramer, J. Polymer Sci. Phys., 20, 899, (1982).
15. H. H. Kausch and M. Dettenmaier, Polymer Bull. 3, 565, (1980).
16. B. Gross, Mathematical Structure of the Theories of Viscoelasticity, Hermann, Paris, (1953).

Fig. 1 Multi-crazes on a Simple Tension Sheet Specimen (Direction of stressing vertical)

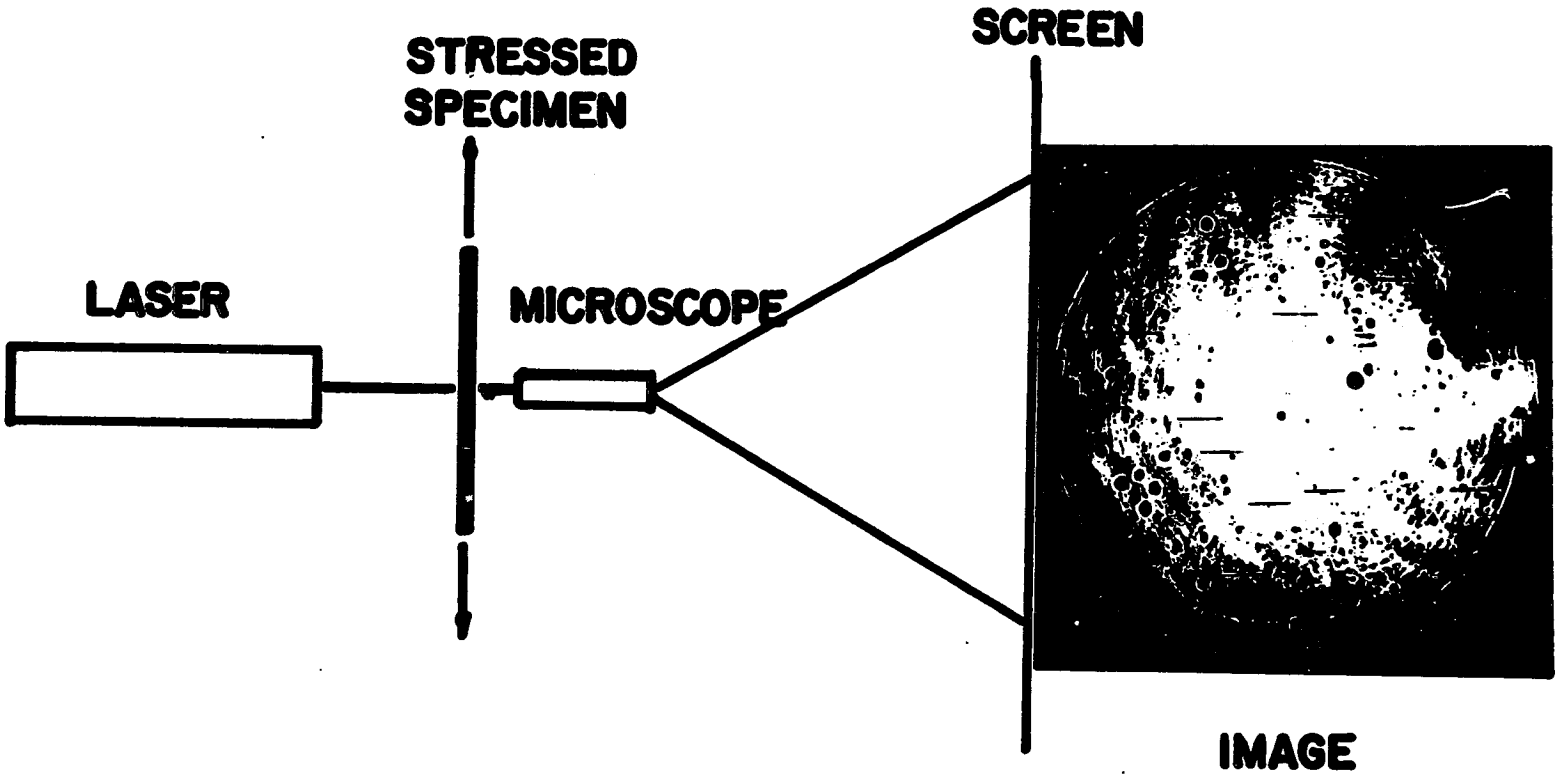

Fig. 2 Experimental set up for Craze Observation

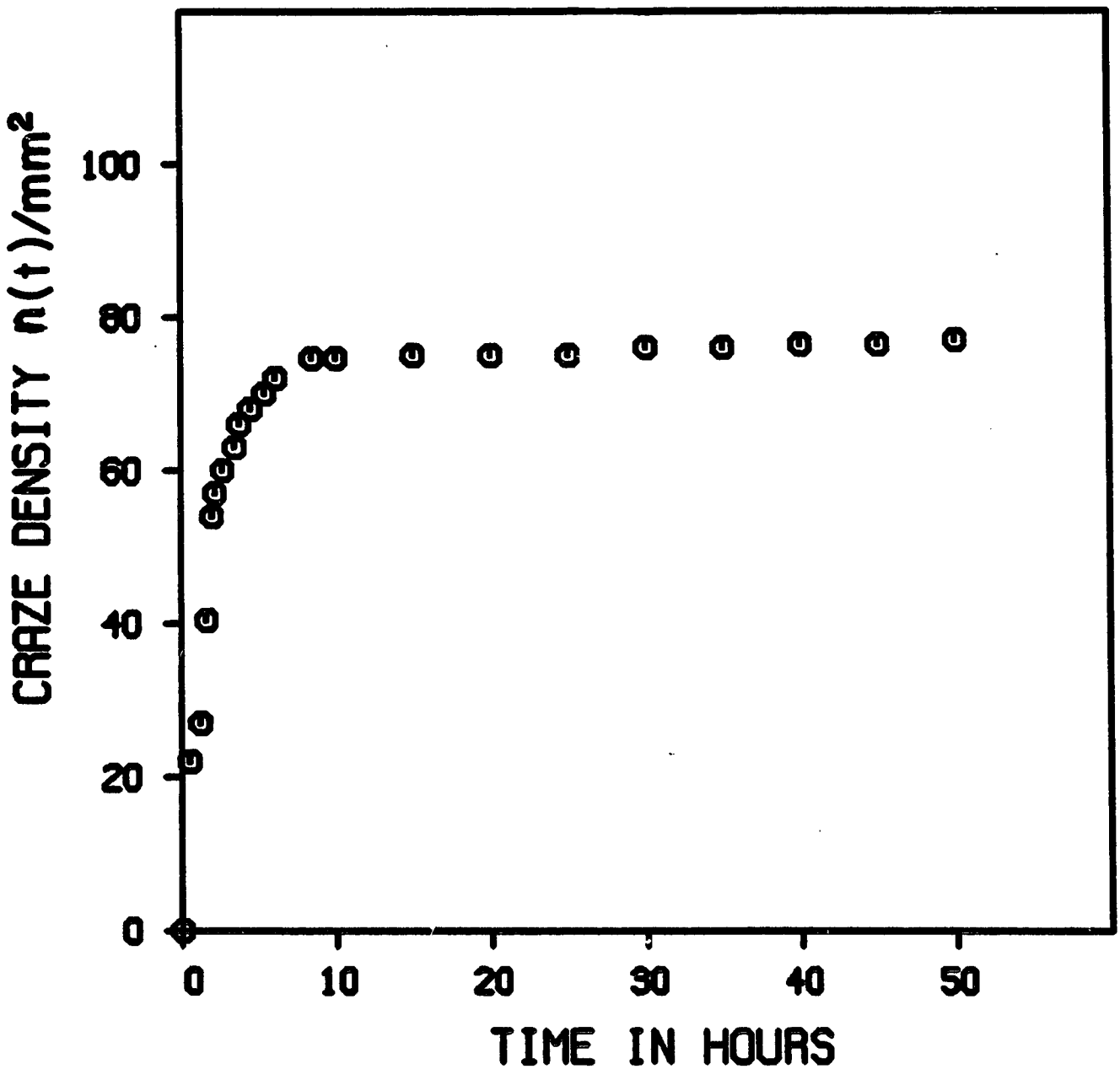

Fig. 3 Number of Craze per unit area vs. Time

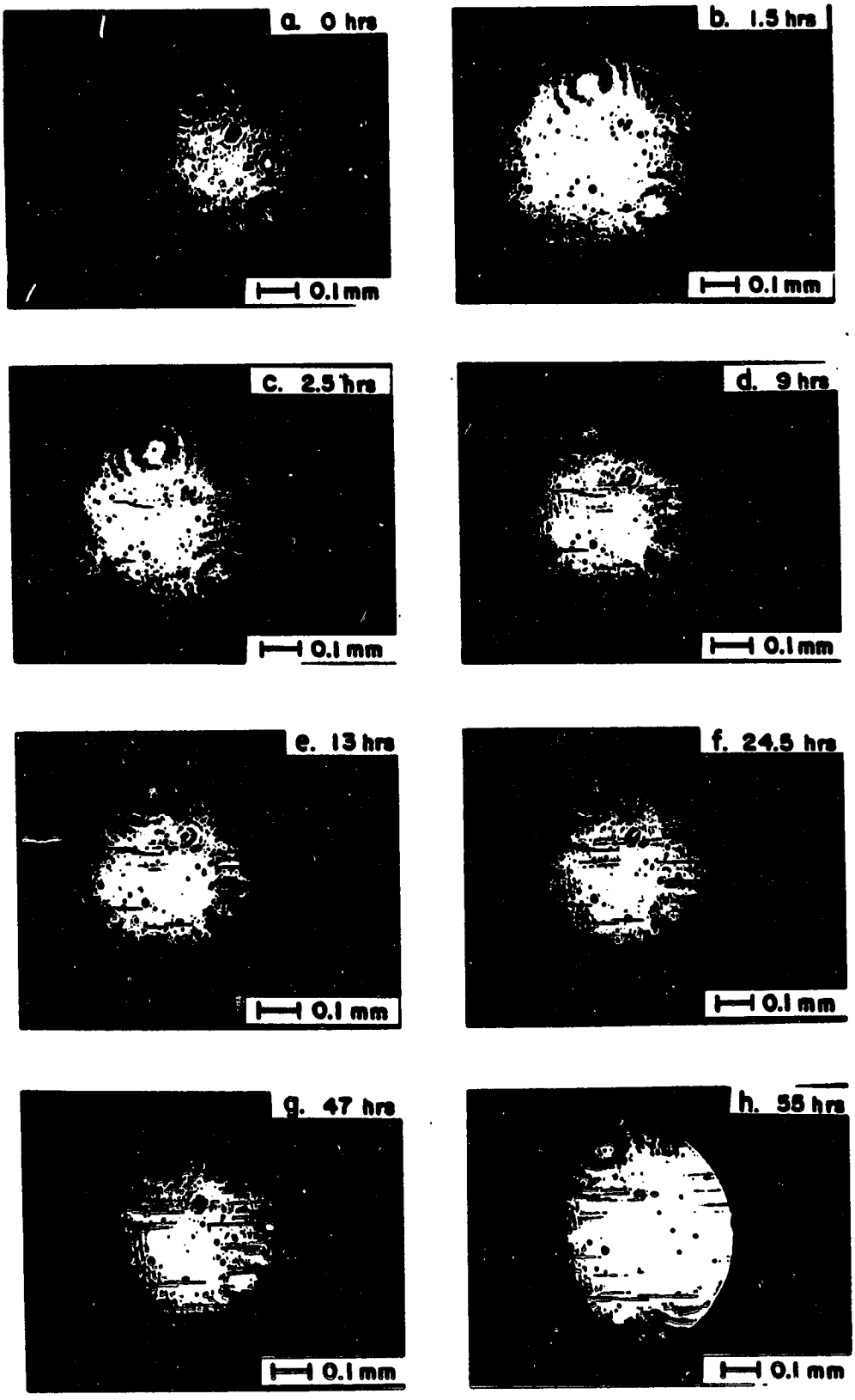

Fig. 4 Craze Propagation in Creep

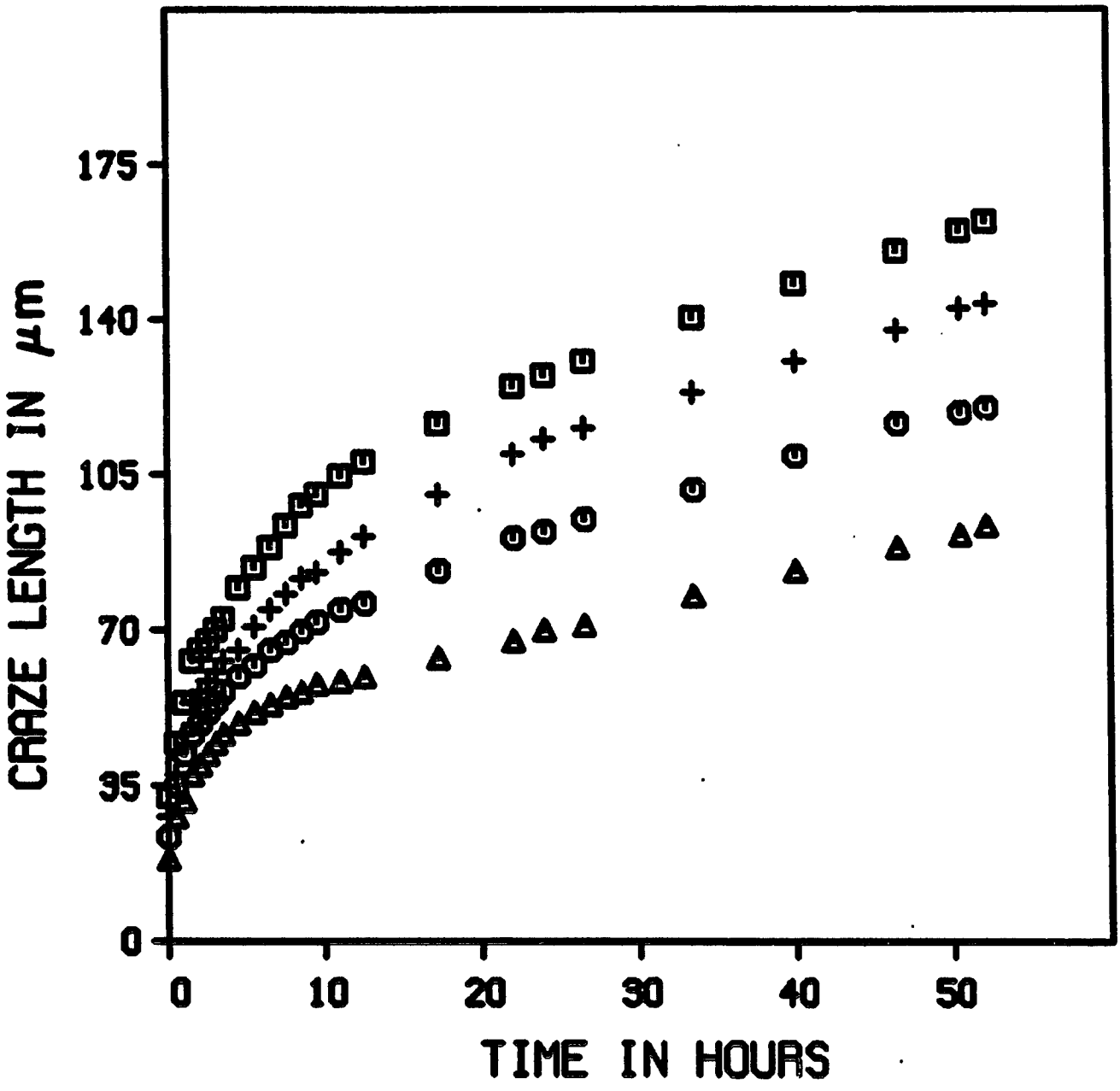

Fig. 5 Experimental Craze Length in Creep

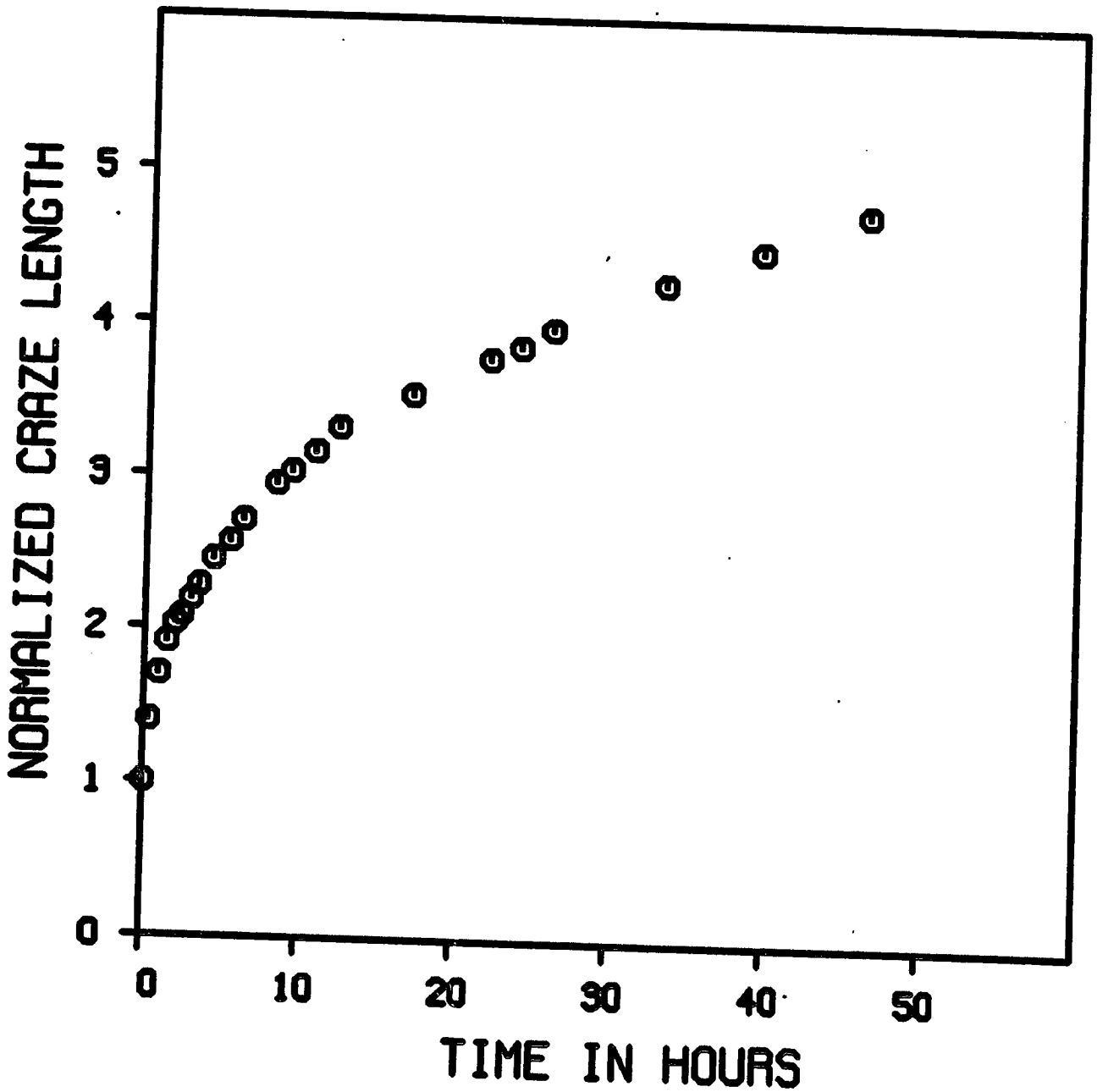

Fig. 6 Typical Craze Length Behavior of a Family of Crazes

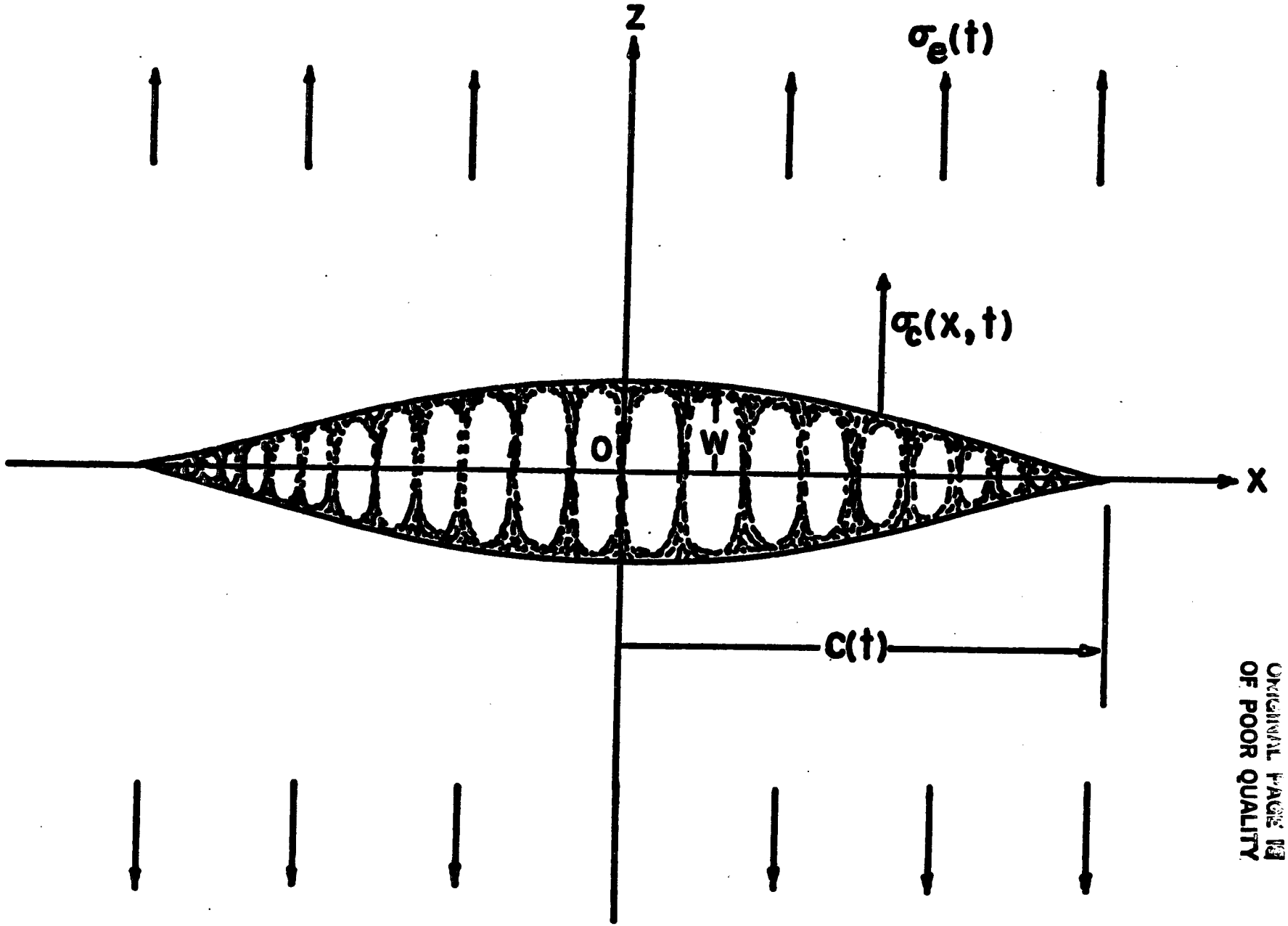

Fig. 7 Schematic Diagram of a Two-Dimensional Craze

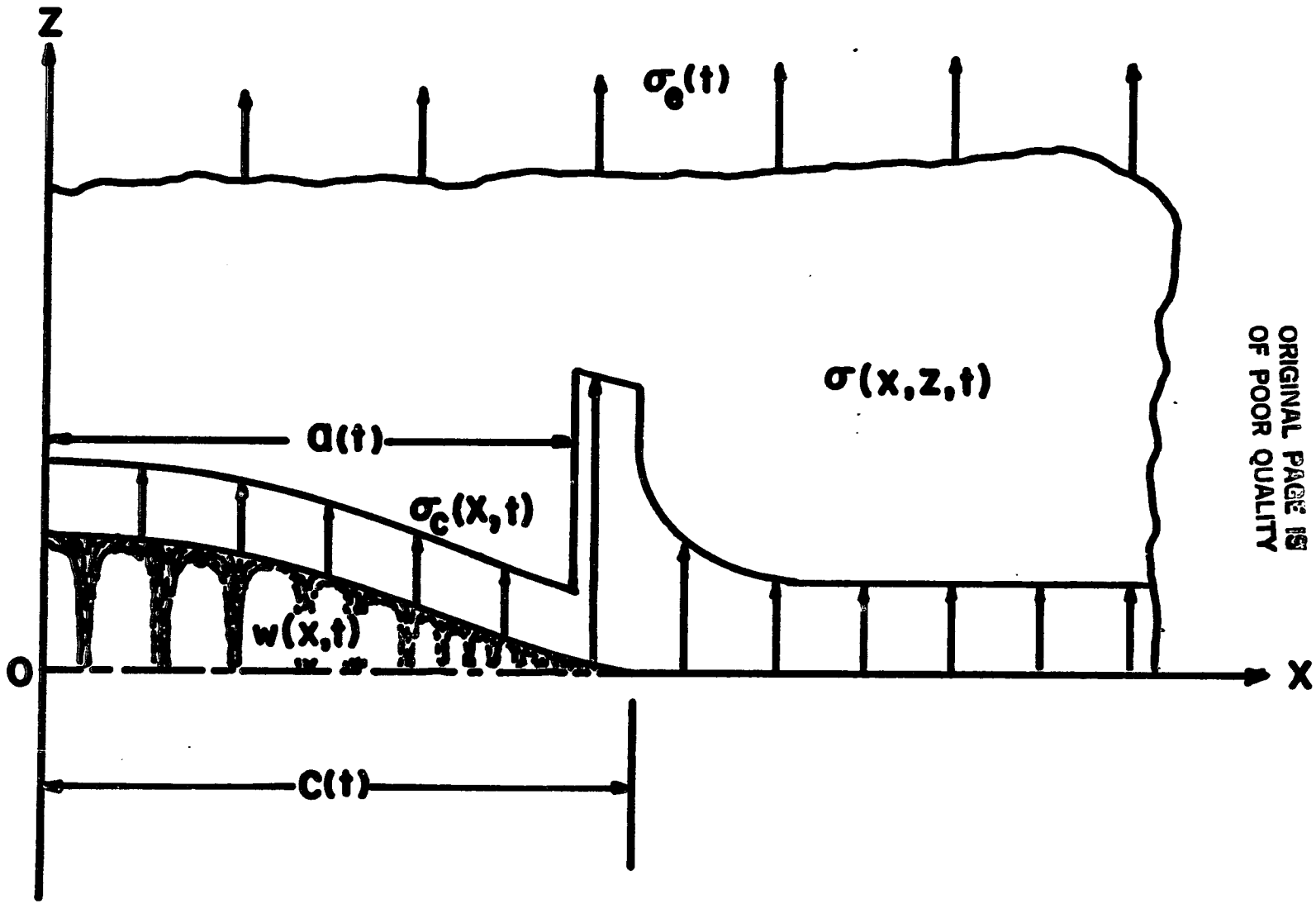

Fig. 8 Two-Dimensional Quadrantal Craze showing a suitable Admissible Craze Envelope Stress

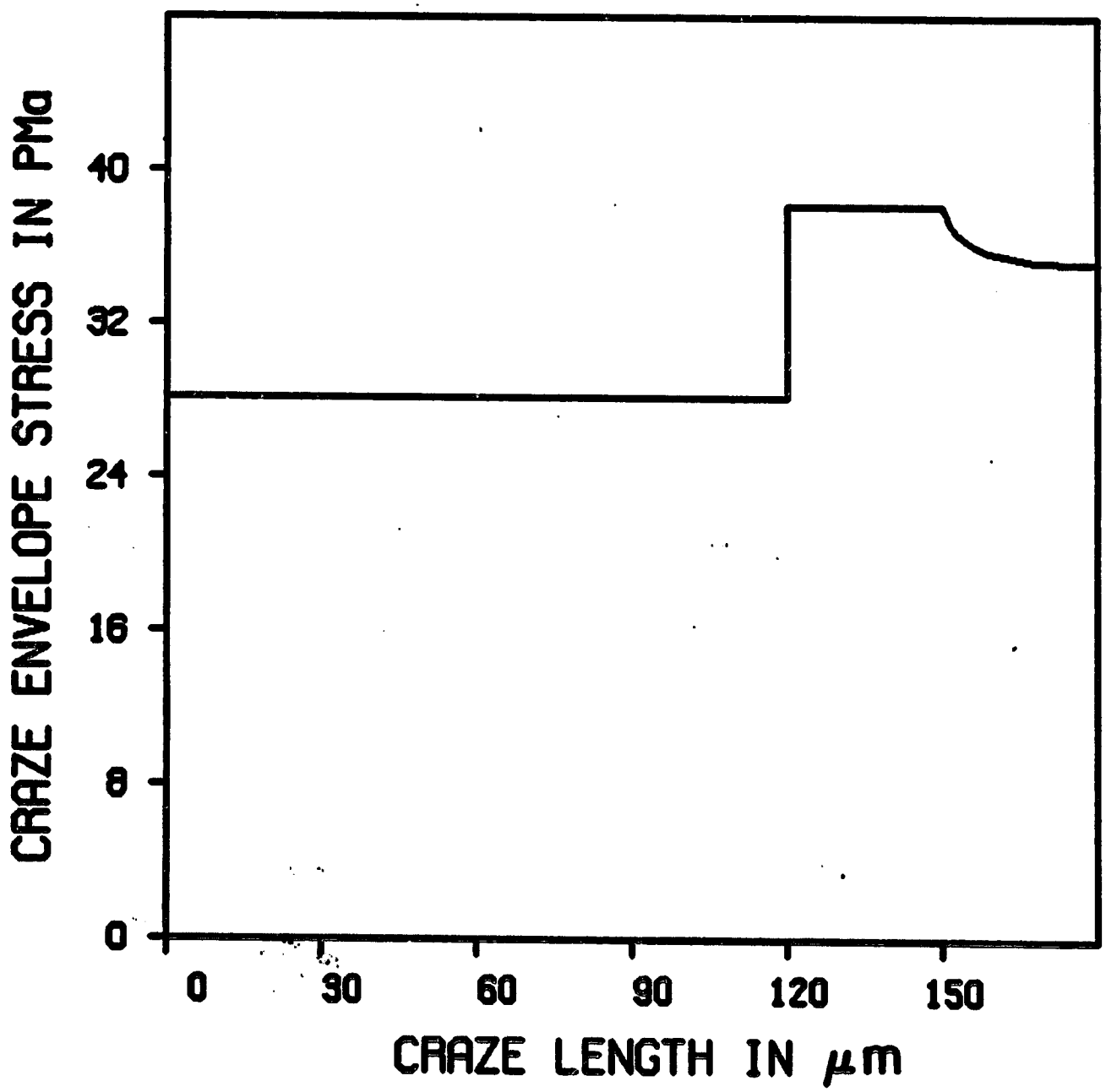

Fig. 9 Craze Envelope Stress Distribution along Craze Length

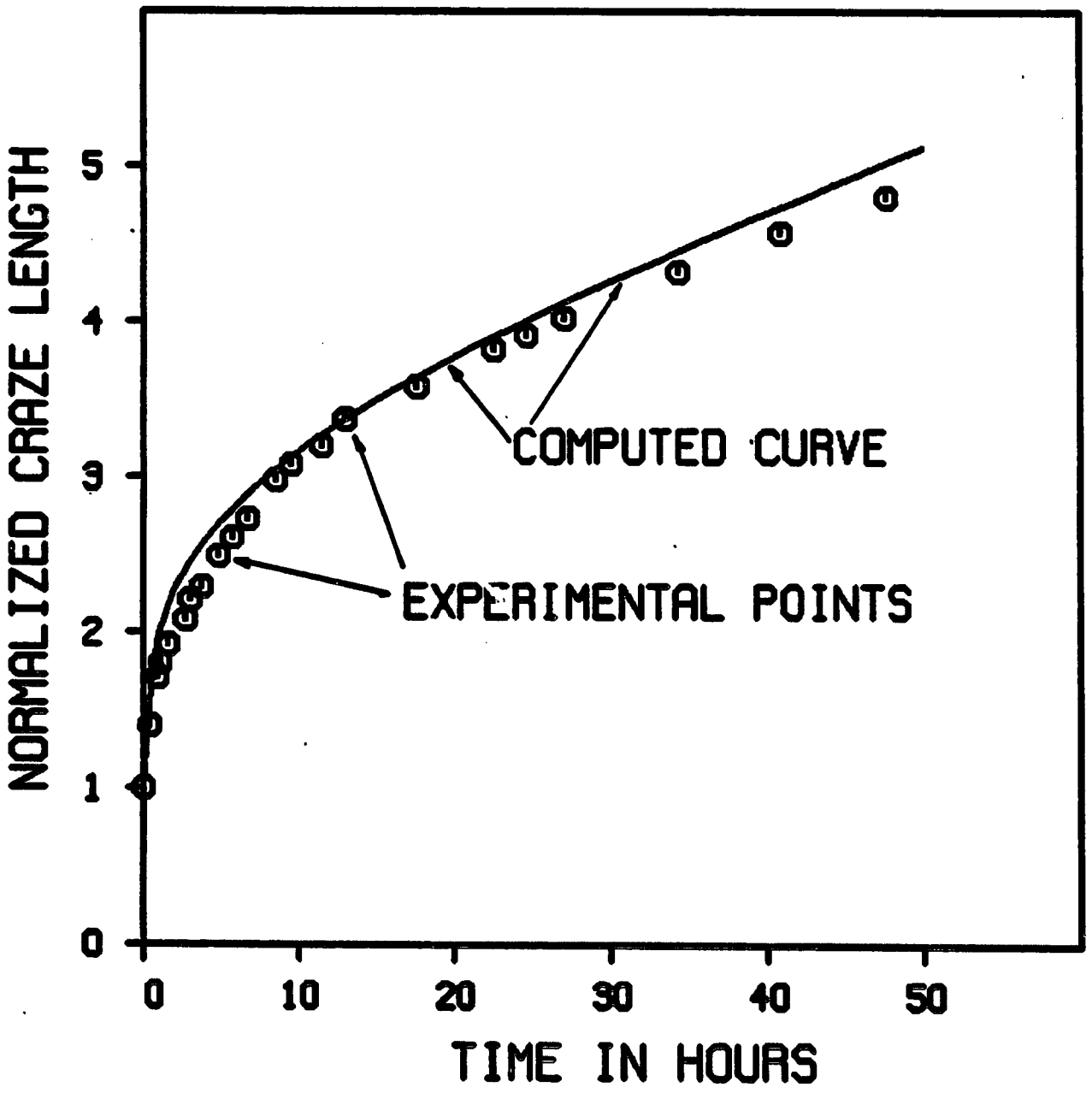

Fig. 10 Comparison of Time Dependent Craze Length in Creep

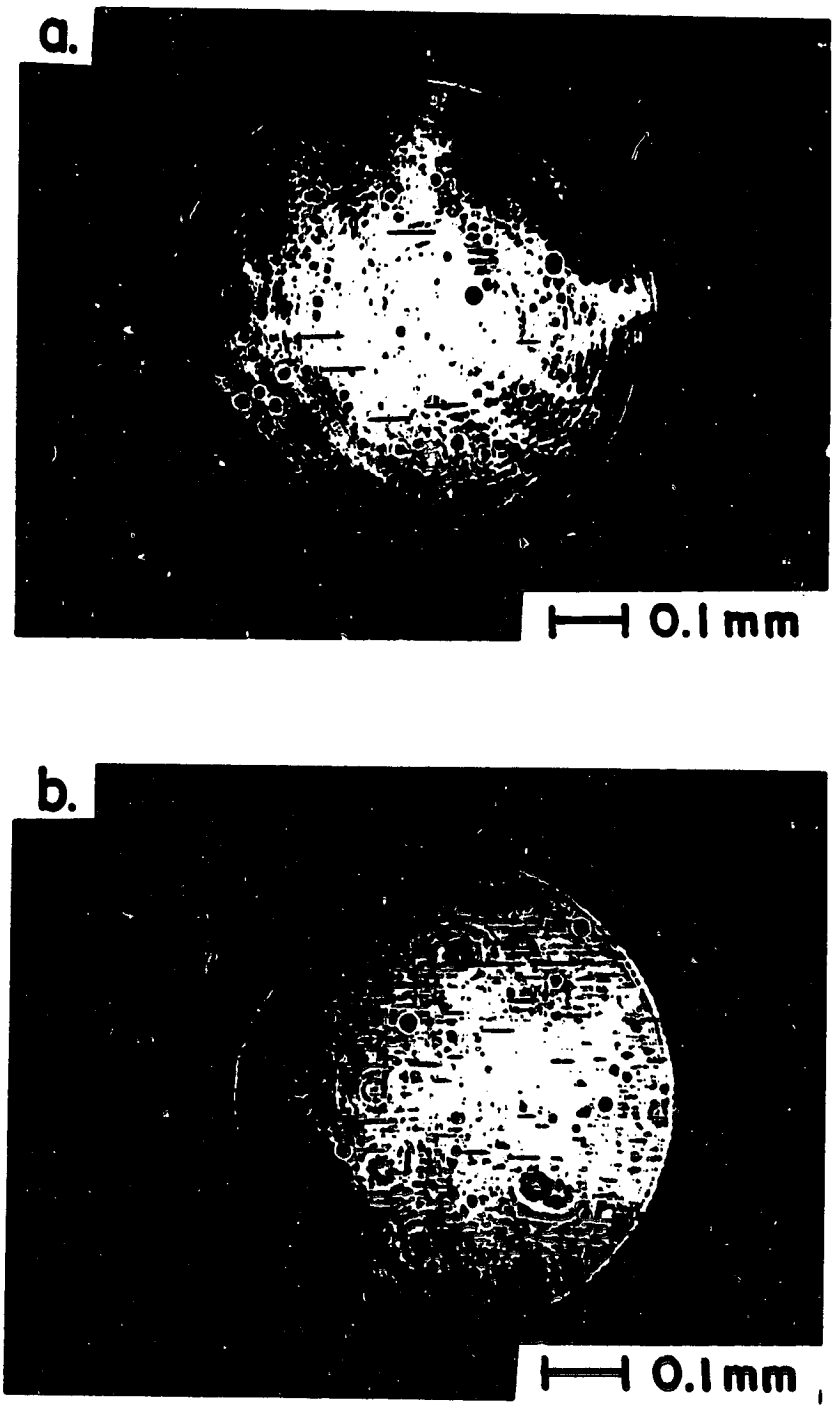

Fig. 11 Load-Time-Craze Relations

a. low load
b. high load

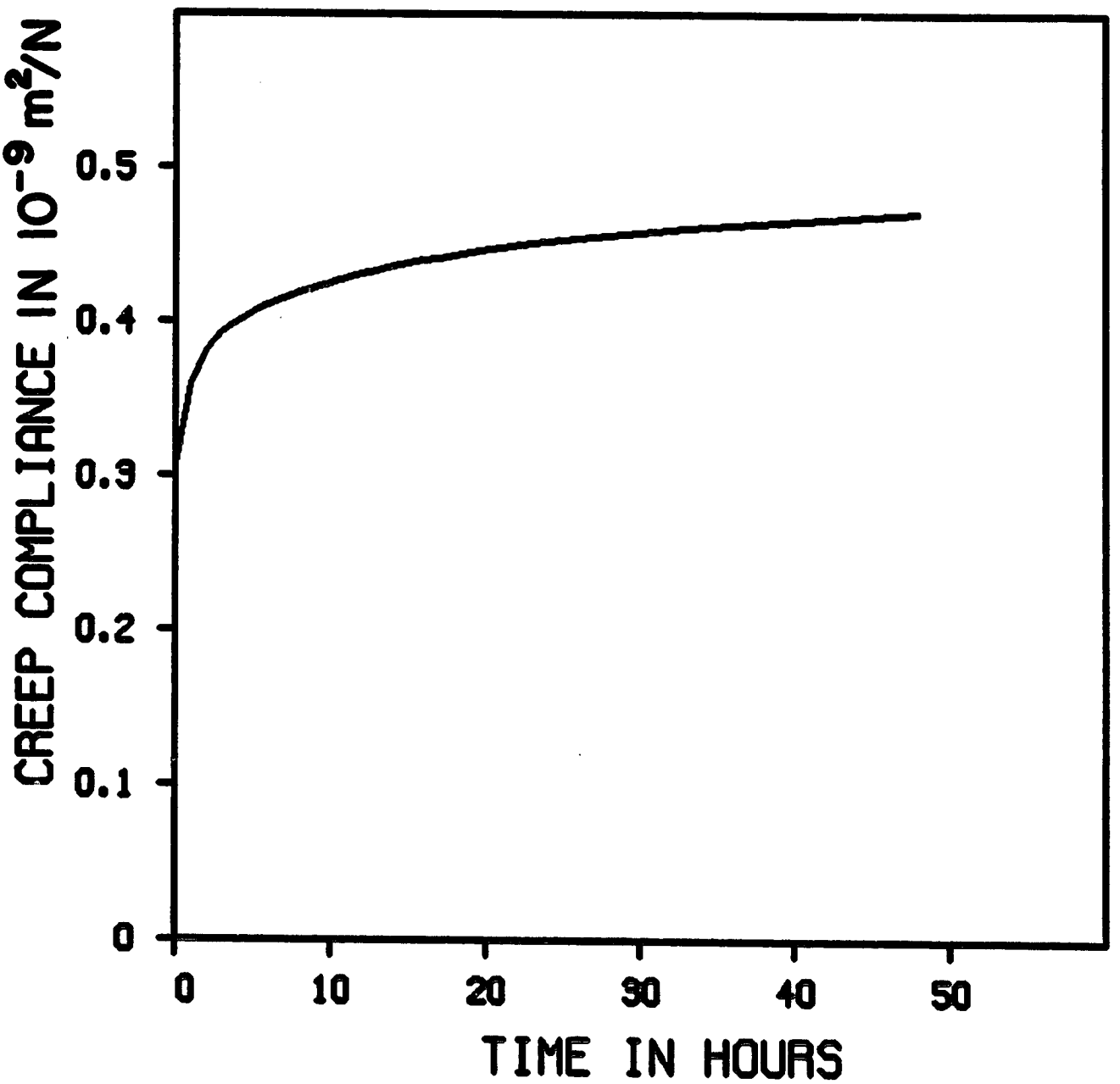

Fig. 12 Creep Compliance for Polystyrene